Drug Design, Development and Therapy

Dovepress
Taylor & Francis Group

Open Access Full Text Article

ORIGINAL RESEARCH

Jiawei Erzhiwan Ameliorates Androgenetic Alopecia by Regulating the SIRT1/JNK/p38 MAPK Pathway

Zhiguang Huang[1,2,*], Yuanyuan Li[3,*], Yixin Xie[1,2,*], Hangjie Fu[2,4], Zhiwei Weng[1,2], Jianchang Yuan[1,2], Lan Wu[1,2], Weizhou Lin[1,2], Yi Cao[3], Bin Ding[1,2,5]

[1]School of Life Sciences, Zhejiang Chinese Medical University, Hangzhou, People's Republic of China; [2]Academy of Chinese Medical Science, Zhejiang Chinese Medical University, Hangzhou, People's Republic of China; [3]The First Affiliated Hospital of Zhejiang Chinese Medical University, Hangzhou, People's Republic of China; [4]School of Public Health, Zhejiang Chinese Medical University, Hangzhou, Zhejiang, People's Republic of China; [5]Jiaxing TCM Hospital Affiliated to Zhejiang Chinese Medical University, Jiaxing, People's Republic of China

*These authors contributed equally to this work

Correspondence: Bin Ding, College of Life Science, Zhejiang Chinese Medical University, No. 548 Binwen Road, Hangzhou, 310053, People's Republic of China, Tel +86 18058107528, Email db@zcmu.edu.cn; Yi Cao, The First Affiliated Hospital of Zhejiang Chinese Medical University, 289 Shanggang Road, Xihu District, Hangzhou, 310060, People's Republic of China, Email caoyi1965@163.com

Purpose: Androgenetic alopecia (AGA) is a type of hair loss. Our previous study showed AGA ameliorating capability of water extract of an herbal prescription, "Jiawei Erzhiwan" (WJWE), which was derived from the traditional formula "Erzhiwan". However, the underlying mechanisms is still unknown.

Patients and Methods: In this study, the phytochemical ingredients in WJWE were characterized via UPLC–MS/MS analysis. The dihydrotestosterone (DHT)-induced murine model and dermal papilla cells (DPCs) assays were used to evaluate and elucidate the beneficial effects and mechanisms of WJWE on AGA.

Results: WJWE promoted hair growth and hair follicle regeneration in AGA mice, improved DPCs growth and dose-dependently protected DHT-reduced DPCs viability in vitro by stimulating the Wnt5A/β-Catenin pathway. Additionally, WJWE reduced DHT-induced oxidative stress in AGA model murine skin and DHT-treated DPCs. To elucidate the regulative mechanism, we found that WJWE treatment significantly and dose-dependently increased the expression of SIRT1 and reduced the phosphorylation of JNK and p38 MAPK in both DHT-treated DPCs and AGA model mice. And the application of EX527 (a SIRT1 inhibitor) could the effect of WJWE.

Conclusion: Our study provided some evidence of WJWE on AGA treatment, by which SIRT1/JNK/p38 MAPK signaling pathway might be the major target.

Keywords: androgenetic alopecia, Erzhiwan, JNK, p38 MAPK, oxidative stress, SIRT1

Introduction

Androgenetic alopecia (AGA) is a multifactorial type of hair loss, characterized by hair follicles miniaturization, in which highly expressed 5-α reductase and excessive sensitivity of the androgen receptor (AR) are the two critical events.[1] The AR in dermal papilla cells (DPCs) reduces the level of β-Catenin by high-affinity binding of dihydrotestosterone (DHT), which is the catalytic product of 5-α Reductase.[2] And β-Catenin leads the expression of growth factors, such as IGF, VEGF et al, which improve the growth of hair follicles.[3] For decades, the incidence of AGA is continually increasing, even among the younger generations. Furthermore, COVID-19 infection can induce alterations in testosterone levels, which may contribute to exacerbating hair loss.[4] It severely impacts the social confidence and psychological health of patients.[5] Topical treatment with minoxidil and oral application of finasteride have been approved by the Food

Received: 5 November 2024
Accepted: 26 March 2025
Published: 1 April 2025

Graphical Abstract

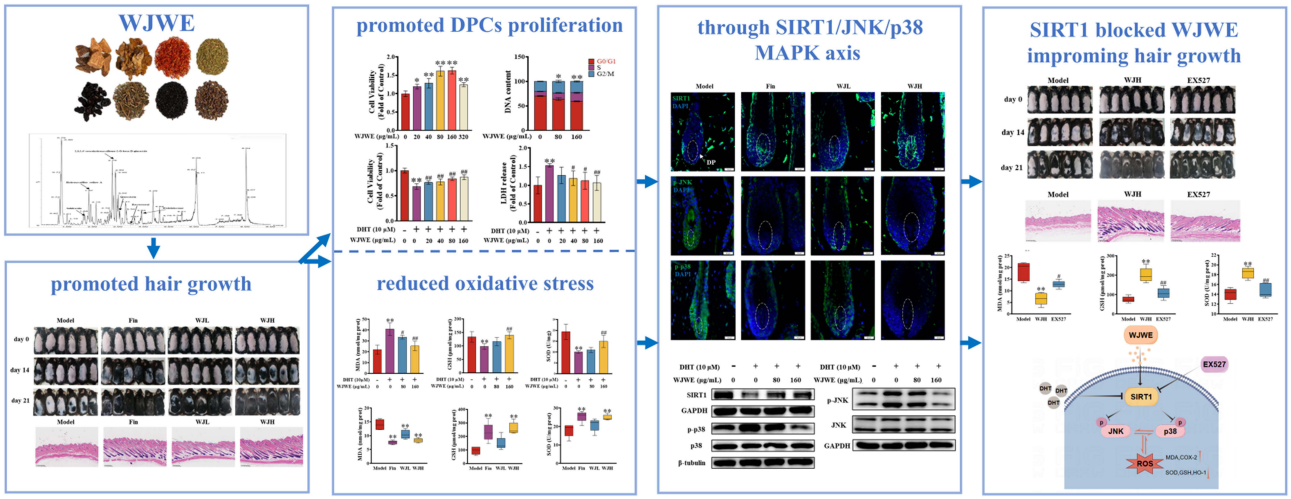

and Drug Administration for AGA treatment. However, the patient compliance and adherence are always problems, because of unwished adverse effects.[6] Therefore, novel therapeutic materials are greatly favored in decades.

Herbs are exploiting in health keeping since ancient time.[7,8] "Erzhiwan" is a traditional Chinese herbal prescription, which is extensively applied to treat diseases, such as hair loss, menstrual disorders and aging.[9–11] "Erzhiwan", originates from "Fu Shou Jing Fang", a medical treatises book in Ming Dynasty, consists of Nvzhenzi (Ligustrum lucidum W.T. Aiton) and Mohanlian (Eclipta prostrata L.), both of which serves as the sovereign drugs of the formula.[12,13] The traditional Chinese medicine practitioners consider that the primary pathogenesis of AGA lies in the imbalance of "Yin" and "Yang" within the "kidney". The simultaneous occurrence of "dampness" "heat" and "kidney Yin" deficiency results an effect ackin of toxins, which "steam" up to the head and influenced the growth of hair.[14] And "Erzhiwan" can balance "Yin" and "Yang" by nourishing Yin, tonifying the kidneys, clearing heat. Even though, we still modified the formula of "Erzhiwan" according to the holism concept of traditional Chinese medicine and the hierarchy to improving the efficiency on AGA treatment. And the novel prescription is "Jiawei Erzhiwan", which consists of eight traditional Chinese herbs: Nvzhenzi (Ligustrum lucidum W.T. Aiton), Mohanlian (Eclipta prostrata L.), Honghua (Carthamus tinctorius L.), Sangshen (Morus alba L.), Heshouwu (Reynoutria multiflora (Thunb.) Moldenke), Huangjing (Polygonatum sibiricum F. Delaroche), Cebaiye (Platycladus orientalis (L.) Franco), and Heizhima (Sesamum indicum L.) (the plant name was checked in the "World Flora Online", www.worldfloraonline.org). And WJWE, in this study, is a lyophilized powder of the water extract of the "Jiawei Erzhiwan". Previously, we have demonstrated the beneficial effect of WJWE on AGA with a case study.[15] However, the phytochemical character and the underlying biological mechanism of WJWE remained unclear.

To our knowledge, sirtuin-1 (SIRT1) is a deacetylase, who plays a key role in cell survival, migration, proliferation, differentiation, and senescence. It has been discovered that SIRT1 promotes the proliferation and migration of hair follicle stem cells (HFSCs).[16] Additionally, it can ameliorate the inflammatory response of hair follicle outer root sheath cells in alopecia areata.[17] Moreover, SIRT1 has been reported to be a key regulator for abnormal oxidative stress amelioration in cells, by which the c-Jun N terminal kinase (JNK) and p38 mitogen activated protein kinases (MAPK) might be two signaling mediators.[18] Moreover, high levels of reactive oxygen species (ROS) can trigger premature senescence of DPCs and influence follicle regeneration.[19] These findings suggested that SIRT1 might be crucial in AGA.

In the present study, we performed the in vitro and in vivo experiments to evaluate the effects of WJWE on AGA, by which Wnt/β-Catenin pathway has been stimulated. And the results also revealed that SIRT1/JNK/p38 MAPK signaling pathway has been regulated by WJWE.

Materials and Methods

Chemicals and Reagents

Dihydrotestosterone (DHT, ID0310), EX527 (S1541) and finasteride (S1197) were sourced from Solarbio (Beijing, China) and Selleck Chemicals (Houston, Texas, USA), respectively. The chemicals, salidroside, hydroxysafflor yellow A, 2,3,5,4′-tetrahydroxystilbene-2-O-beta-D-glucoside, quercitrin, resveratrol, and wedelolactone were purchased from Yuanye Biological Technology Co., Ltd. (Shanghai, China). Anti-β-Catenin (A00004), anti-K15 (BM4260), anti-β-actin (MA1115), anti-GAPDH (M00227), and anti-β-Tubulin (M05613-4) antibodies were obtained from Bosterbio (Pleasanton, CA, USA). Additionally, anti-SIRT1 (2028), anti-p38 MAPK (9212), anti-phospho-p38 MAPK (4511), anti-SAPK/JNK (9255), anti-phospho-SAPK/JNK (9258), anti-HO-1 (43966) antibodies were purchased from Cell Signaling Technology (Danvers, MA, USA). An anti-Wnt5A antibody (sc-365370) was applied by Santa Cruz Biotechnology (CA, USA). The anti-COX-2 antibody (ab179800) was purchased from Abcam (Cambridge, UK). RIPA lysis buffer (P0013), BCA protein assay kit (P0011), rapid blocking buffer (P0252), and enhanced chemiluminescence (P0018) reagents were obtained from Beyotime Biotechnology (Shanghai, China).

Preparation and Characterization of the WJWE

All the herbal materials were obtained from the Chinese Herbal Pieces Factory of Zhejiang Traditional Chinese Medicine Hospital (Hangzhou, China). The herbs, Nvzhenzi, Mohanlian, Honghua, Sangshen, Heshouwu, Huangjing, Cebaiye, and Heizhima were mixed with the weight ratio of 12:12:10:10:10:9:6:6. Then, the 75-gram herbal mixture was then steeped in 1.5 L distilled water for 30 min and extracted with a reflux extraction device for 2 h. This herbal mixture was extracted with boiling water twice. The filtrated aqueous fractions were collected, mixed, and concentrated with a vacuum-pumped rotary evaporator (BUCHI, Switzerland). Finally, this extremely concentrated extract was lyophilized with a freeze dryer (LaboGene, Lillerød, Denmark) and stored in a refrigerator at −20°C.

In this study, we employed UPLC/MS/MS to characterize and identify the phytochemicals in WJWE. An ACQUITY Premier UPLC system (Waters, Milford, MA, USA) and a BEH C18 column (2.1 mm × 100 mm, 1.7 μm) were used for chromatographic separation. Gradient elution was performed using 0.1% formic acid in water (mobile phase A) and acetonitrile (mobile phase B) as follows: 0–0.2 min, 10% B; 0.2–5 min, 10–60% B; 5–6 min, 60–100% B; and 6–8 min, 100–10% B; at a flow rate of 0.3 mL/min. The injection volume was 1 μL, and the column temperature was 35°C.

Xevo TQ-XS Triple Quadrupole mass spectrometer (Waters, Milford, MA, USA) with an ESI source and multiple reaction monitoring (MRM) mode was used to perform mass spectrometry. In negative mode, results from full -scan mass spectrometry were collected. The MS2 scan range was 50 to 1500, and the full scan range was 50 to 1000. The capillary voltage was 2.5 kV in (+) mode; the source temperature was 150°C; the desolvation temperature was 450°C; and the dwell time was 0.25 ms. The collision gas was argon, while the nebulizer and heater gas were nitrogen (1000 L/h).

AGA Murine Model Preparation and Grouping

6-week-old C57 BL/6 male mice were procured from the Shanghai SLAC Laboratory Animal Co. and all animal experiments were approved by the Animal Care and Ethics Committee of Zhejiang Chinese Medical University (approval number: IACUC-20221128-05) and following the ARRIVE guidelines. According to the Guide for the Care and Use of Laboratory Animals, animal experiments were conducted under appropriate conditions, including a temperature of 20 ± 2°C, 55 ± 5% humidity, and a 12-hour light–dark cycle, freely access to food and water.

The AGA model mice were optimized as previously described.[20] In brief, dorsal hair of 7-week-old male mice was removed using an electric shaver and depilatory cream to induce growth phase entry. All the mice were intraperitoneally injected with 200 μL of 1 mg DHT (10% DMSO, 40% PEG300, 5% Tween 80 and 45% saline) on days, 1, 3, 5, 15, and 17. To evaluate the hair growth promoting activity of WJWE, the mice were randomly divided into four groups (6 mice in each group); the model group (Model), finasteride group (Fin), WJWE low-dose group (WJL), and WJWE high-dose group (WJH). The mice in the model group were intragastrically administered 200 μL of H2O every day. The mice in the Fin group were intragastrically administered 10 mg/kg finasteride in 200 μL of H2O per day. The WJL and WJH mice intragastrically received 100 mg/kg and 200 mg/kg WJWE, in 200 μL of H2O per day, respectively.

To identify SIRT1 as the key target of WJWE, the mice were separated into three groups: the model and WJH groups, as well as the EX527 group. The mice modeling and treatment in the model and WJH groups were performed according to the methods. The mice in the EX527 group were intragastrically administered 200 mg/kg WJWE per day and subcutaneously injected with 5 mg/kg EX527 in 200 μL of solvent (10% DMSO, 40% PEG300, 5% Tween 80 and 45% saline) in every 5 days during the experiment. We recorded hair growth on the depilated dorsal skin with a digital camera on days 1, 14, and 21. At the end of the experiment, the blood and dorsal skin of the mice in the different groups were collected for further analysis.

Morphological and Histological Study

The dorsal skin of mice, fixed in 4% paraformaldehyde, was dehydrated and embedded in paraffin. Then, the embedded skin sections were sliced, deparaffinized, and stained with hematoxylin and eosin (H&E) reagents (BOSTER, Beijing, China). The sections were photographed with a microscope (Olympus, Tokyo, Japan).

For immunohistochemistry staining, the tissue sections were deparaffinized and incubated in citrate buffer for antigen retrieval. The sections were then treated with a 3% hydrogen peroxide solution. Following this, the sections were incubated at room temperature with 10% goat serum for 30 minutes. The skin slices were subsequently incubated overnight at 4°C with the primary antibody (1:200). After PBS washes, HRP-conjugated secondary antibodies were applied for 1 hr at RT. Diaminobenzidine (DAB) chromogen was used for signal development. The sections were then counterstained with hematoxylin and sealed. Finally, the stained sections were imaged using a Digital Slice Scanner (Nikon Corporation, Tokyo, Japan).

For immunofluorescence staining, the tissue sections were deparaffinized, followed by citrate buffer incubation to retrieve the antigen. After being blocked with 10% goat serum, the skin slices were incubated overnight at 4°C with primary antibody (1:200). The following day, a fluorescently labeled secondary antibody (1:200) was applied to combine with antibody, and the nuclei were simultaneously visualized via DAPI staining. Finally, these skin slices were imaged via fluorescence microscopy (Nikon Corporation, Tokyo, Japan).

DHT Content Measurement

Sera DHT levels were measured with a dihydrotestosterone ELISA kit (JM-028014M1, Jiangsu Jingmei Biological Technology Co. Ltd., Jiangsu, China), according to the manufacturer's instructions.

Cell Culture and Treatment

Immortalized Hair Follicle Dermal Papilla Cells (DPCs) were obtained from Meisen CTCC (CTCC-001-0426, Zhejiang, China) and tested negative for mycoplasma contamination. These cells were cultured in complete medium and grown in a humidified atmosphere container with 5% CO2 at 37°C. When the cell culture in the flask reached 85–90% confluence, the cells were then seeded into either 96-well or 6-well plates to grow overnight for tests. The in-well-grown cells were treated with different concentrations of WJWE (0, 20, 40, 80, 160, and 320 μg/mL) for 24 h. For DHT-induced experiments, the in-well -grown cells were first treated with either 0.01% DMSO or 10 μM DHT for 2 h, and then incubated with various concentrations of WJWE for 24 h.

Cell Viability, Cell Cycle and Extracellular Lactate Dehydrogenase (LDH) Levels Assay

Cell viability, cell cycle, and the extracellular LDH were assessed using specific kits: CCK-8 assay kit (CK04), cell cycle assay kit (C543), and cytotoxicity LDH assay kit (CK12), respectively, which were purchased from Dojindo (Kumamoto, Japan). The detection methods were conducted following the manufacturer's instructions, with a microplate reader (Thermo Fisher Scientific, MA, USA) or a flow cytometer (BD Biosciences, San Jose, CA, USA).

DPPH Assay

The radical scavenging activity of WJWE was evaluated with a 2,2-diphenyl-1-picrylhydrazyl (DPPH) assay kit (A153-1-1, Nanjing Jiancheng Co., Ltd., Nanjing, China). Briefly, 1 mg/mL WJWE water solution was gradually diluted with 80% methanol to obtain detection solutions with concentrations of 40, 80, 160 and 320 μg/mL. Then, WJWE solutions were mixed with the DPPH working solution and incubated in the dark at room temperature for 30 min. Absorbance were taken at 517 nm using an

ultraviolet–visible spectrophotometer (Shanghai Instrument and Electricity Analysis Co., Ltd., Shanghai, China). The 80% methanol solution, as well as 100 μg/mL vitamin C in 80% methanol, was used as a blank and positive control, respectively.

Oxidative Stress Determination

The tested murine skin or DPCs were lysed with RIPA lysis solution or an appropriate buffer solution at 4°C and then centrifuged to collect the supernatant. The contents of superoxide dismutase (SOD), glutathione (GSH) and malondialdehyde (MDA) were determined via the specific kits from Nanjing Jiancheng Co., Ltd. (A001-3-2, A006-2-1, A003-1-2, Nanjing, China), according to the manufacturers' instructions.

ROS level in DPCs was measured by flow cytometry. Briefly, the cells in different assays were incubated with 5 μM DCFH-DA (S0033, Beyotime Biotechnology, Shanghai, China) at 37°C for 30 minutes. After washing with PBS buffer, the cells were analyzed using a flow cytometer (BD Biosciences, San Jose, CA, USA).

Western Blotting Assay

Skin tissues or DPCs were lysed with RIPA lysis buffer, and the proteins were collected by centrifugation. Protein concentration in the lysate was determined with a BCA protein assay kit. Subsequently, 40 μg protein was separated by SDS-PAGE (8–12%) and transferred onto PVDF membranes (Millipore, Massachusetts, USA) via electrophoresis. After a 20 minutes incubation with rapid blocking buffer, the membranes were treated with the specific primary antibodies overnight at 4°C. The following day, the membranes were washed with TBST and hybridized with the appropriate secondary antibody for 1 h. The specific luminous signal was developed with enhanced chemiluminescence reagents and recorded with a chemiluminescence imaging analysis system (Tanon, China).

Quantitative Real-Time Polymerase Chain Reaction (qRT–PCR)

Total RNA was isolated via the TRIzol method (15596026, Thermo Fisher Scientific, Waltham, MA, USA). The RNA was subsequently reverse transcribed with ReverTra Ace® qPCR RT Master Mix (QPX-201, TOYOBO, Osaka, Japan). For each qRT–PCR assay, 50 ng of the reverse transcribed product was used as template and mixed with Fast Mix Quantitative RT–PCR Master Mix (MQ10201S, Monad, Suzhou, China) as well as the specific primers in a total volume of 20 μL. Amplification and real-time analysis were performed on a Step One Plus System (Applied Biosystems, Waltham, MA, USA). The primer sequences are listed in Table 1.

Statistical Analysis

The data are presented as means ± SDs and were analyzed using GraphPad Prism 9.0. Differences among multiple groups were evaluated using one-way ANOVA, and comparisons between two groups were made using unpaired Student's *t*-test. For datasets with fewer than five samples (limited samples), a permutation test method was used. A p-value < 0.05 was considered statistically significant.

Table 1 The Primers Sequence

Gene	Forward	Reverse
Lef1	TGTTTATCCCATCACGGGTGG	CATGGAAGTGTCGCCTGACAG
Vegf	CTGCCGTCCGATTGAGACC	CCCCTCCTTGTACCACTGTC
Igf1	CTGGACCAGAGACCCTTTGC	GGACGGGGACTTCTGAGTCTT
Gapdh	AGGTCGGTGTGAACGGATTTG	TGTAGACCATGTAGTTGAGGTCA

 https://doi.org/10.2147/DDDT.S501823

Results

Identification of Active Compounds in WJWE

The base peak intensity (BPI) chromatogram obtained in (ESI-) negative ionization mode is shown in Figure 1A. According to the Pharmacopoeia of the People's Republic of China (2020), we selected six ingredients, salidroside, hydroxysafflor yellow A, 2,3,5,4′-tetrahydroxystilbene-2-O-beta-D-glucoside, quercitrin, resveratrol, and wedelolactone, as standards to identifying the chemicals in WJWE. The total ion current chromatograms (TICs) are shown in Figure 1B and C. The ion pair information, retention times, and collision energies of the 6 standard compounds are shown in Supplementary Table 1. The concentrations of salidroside, hydroxysafflor yellow A, 2,3,5,4′-tetrahydroxystilbene-2-O-beta-D-glucoside, quercitrin, resveratrol, and wedelolactone in the WJWE were comparatively determined according to the peak area, which were 1.4 mg/g, 0.791 mg/g, 0.838 mg/g, 0.252 mg/g, 0.085 mg/g, and 0.449 mg/g, respectively.

WJWE Promoted Hair Growth in AGA Model Mice

Our study assessed the significant effect of high-dose WJWE (WJH) and finasteride on hair growth in DHT-induced AGA mice in 14 days. In comparison, no obvious changes were observed in the Model and WJL groups. At the end of this experiment, we also observed significant growth of the dorsal hairs in the WJL group but rarely in the Model group (Figure 2A). The H&E staining images of dorsal skin in different groups also showed few hair follicles in the Model group. In comparison, the WJH and Fin groups obviously represented increased hair follicles density and skin thickness (Figure 2B–D). Since DHT-mediated AGA is linked to Wnt/β-catenin pathway suppression and HFSCs dysfunction ($K15^+$ marker).[21] Therefore, we comparatively assessed the serum DHT concentration and the expression of K15, Wnt5A and β-Catenin in various groups of mice. Compared with those in the Model group, DHT levels in the serum of WJL, WJH and Fin mice were significantly decreased (Figure 2E), and an opposite tendency of K15 (in red) (Figure 2F). We also observed significantly high levels of Wnt5A and β-Catenin in the WJH and Fin groups (Figures 2G and S1A). Transcriptional activation of downstream targets (*IGF1, LEF1, VEGF*) was also observed in WJWE-treated groups (Figure S1B). In summary, WJWE effectively promoted hair growth in DHT-induced AGA model mice, in which the highly level of K15, Wnt5A, and β-Catenin, as well as the increased transcription of IGF1, LEF1 and VEGF were observed.

WJWE Promoted DPCs Proliferation and Alleviated DHT-Induced Cell Damage

Given the critical role of DPCs in regulating HFSCs via Wnt signaling, we investigated WJWE's direct effects on DPCs viability and DHT-induced cytotoxicity. The results of the CCK8 assay revealed a gradually increased cellular viability of DPCs with increasing concentration of WJWE (from 0 to 160 μg/mL). As expected, no cytotoxic effects were observed, even in 320 μg/mL WJWE treated DPCs assay (Figure 3A). We also found obviously increased S and G2/M phases of DPCs, as well as the decreased G1/G0 phases of cells in WJWE (80 and 160 μg/mL) treated assays, with a dose-dependent manner (Figure 3B and C). The proliferation of DPCs plays a crucial role in hair growth cycling, which is the target of DHT.[22] Hence, we investigated the protective ability of WJWE (20, 40, 80 and 160 μg/mL) on DHT treated DPCs. We found significantly and gradually restored cell viability, and gradually decreased LDH in 40, 80 and 160 μg/mL WJWE treated DHT-DPCs assays treated (Figure 3D and E). Moreover, the expression of Wnt5A and β-Catenin were also significantly increased (Figure 3F). These results indicated that WJWE could promote the proliferation of DPCs and mitigate the cytotoxic effect of DHT on DPCs. And in the following experiment we tried to elucidate the underlining mechanism.

WJWE Reduced DHT-Stimulated Oxidative Stress

A previous study suggested that DHT trigged oxidative stress, particularly in DPCs, played the key role in the pathogenesis of AGA.[23] Hence, restoring the oxidative balance in DPCs can attenuate AGA. Therefore, we identified the antioxidative activity of WJWE with DPPH assays. And the results showed that the amount of free DPPH radicals decreased in the assays with WJWE dose dependently. In comparison, 160 and 320 μg/mL WJWE had very similar efficiencies of 100 μg/mL vitamin C (VC) (Figure 4A). The beneficial effects of WJWE (80 and 160 μg/mL) on DHT-

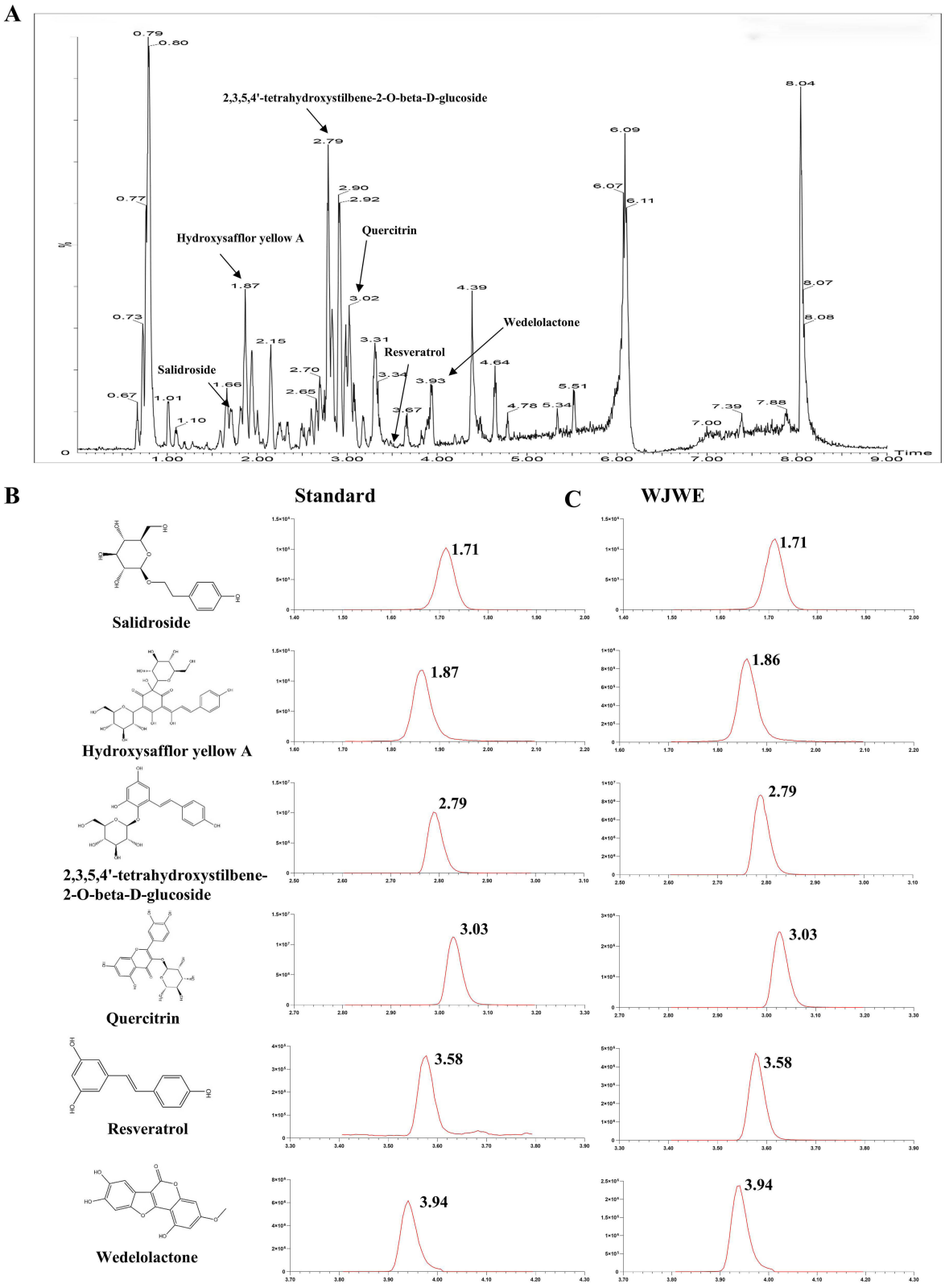

Figure 1 The chemical profile of WJWE was characterized with UPLC-MS/MS. (**A**) The base peak intensity (BPI) chromatogram in negative ion modes; (**B**) the 2D molecular structure and retention time of standards, salidroside, hydroxysafflor yellow A, 2,3,5,4′-tetrahydroxystilbene-2-O-beta-D-glucoside, quercitrin, resveratrol, and wedelolactone; (**C**) the retention time of the six ingredients in WJWE.

https://doi.org/10.2147/DDDT.S501823

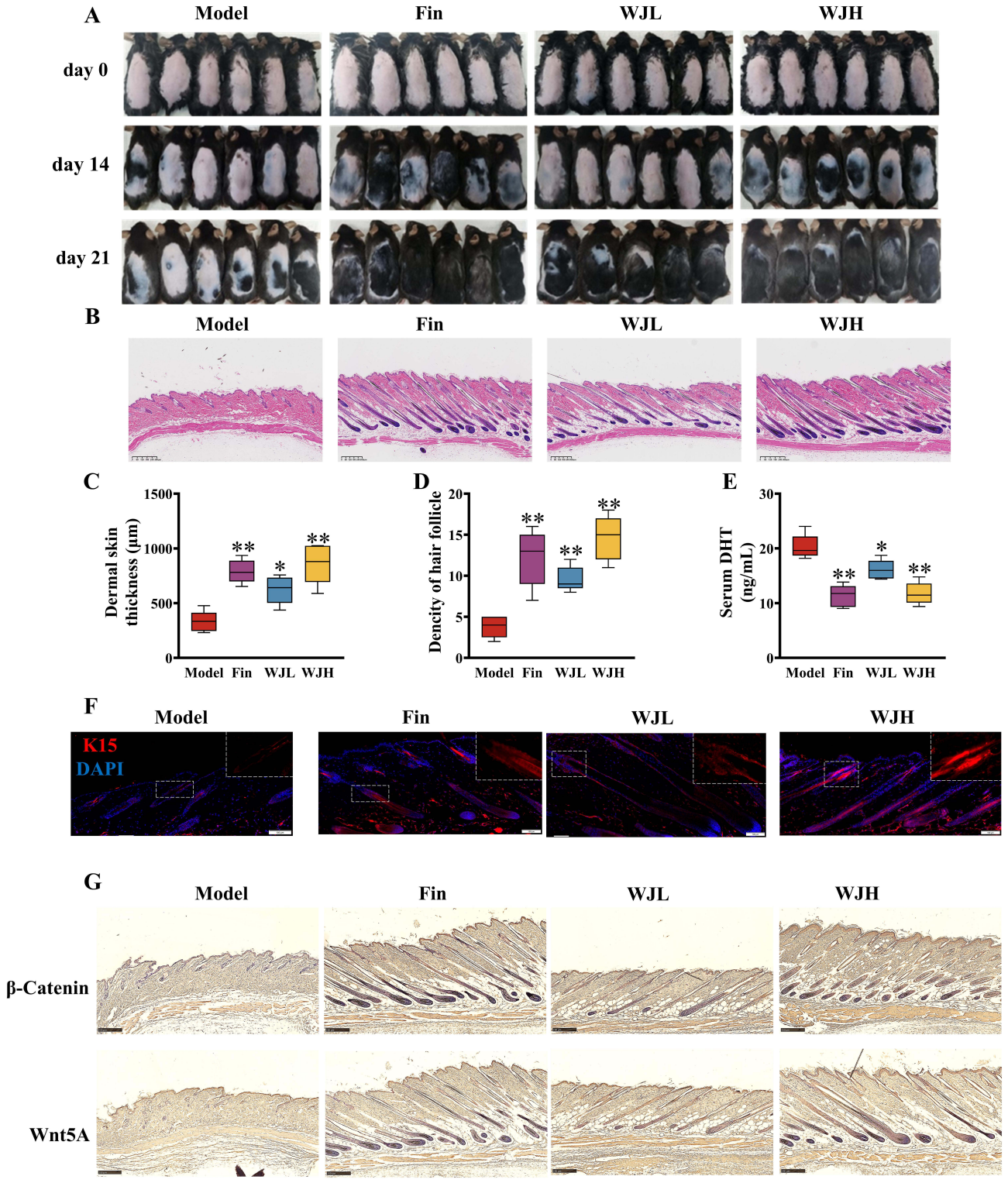

Figure 2 The amelioration capability of WJWE on DHT induced AGA model mice has been evaluated. (**A**) the photographs of dorsal skins in different groups on days 0, 14, and 21 (n ≥ 5); (**B**) the H&E stained skin section of different group mice on day 21, by which the hair follicle could be observed (scale bars = 300 μm, n = 5); (**C**) the quantitative analyses (n = 5) of the skin thickness and (**D**) the density of hair follicle; (**E**) the content of DHT in serum. (**F**) the immunofluorescence stained K15 in the dorsal skin slices in different groups (scale bars = 50 μm, n = 5); (**G**) the expression of β-Catenin, Wnt5A in dorsal skins of mice in different groups (scale bars = 250 μm, n = 5). Results are presented as means ± SEM. *p < 0.05, **p < 0.01, vs Model group.

 https://doi.org/10.2147/DDDT.S501823

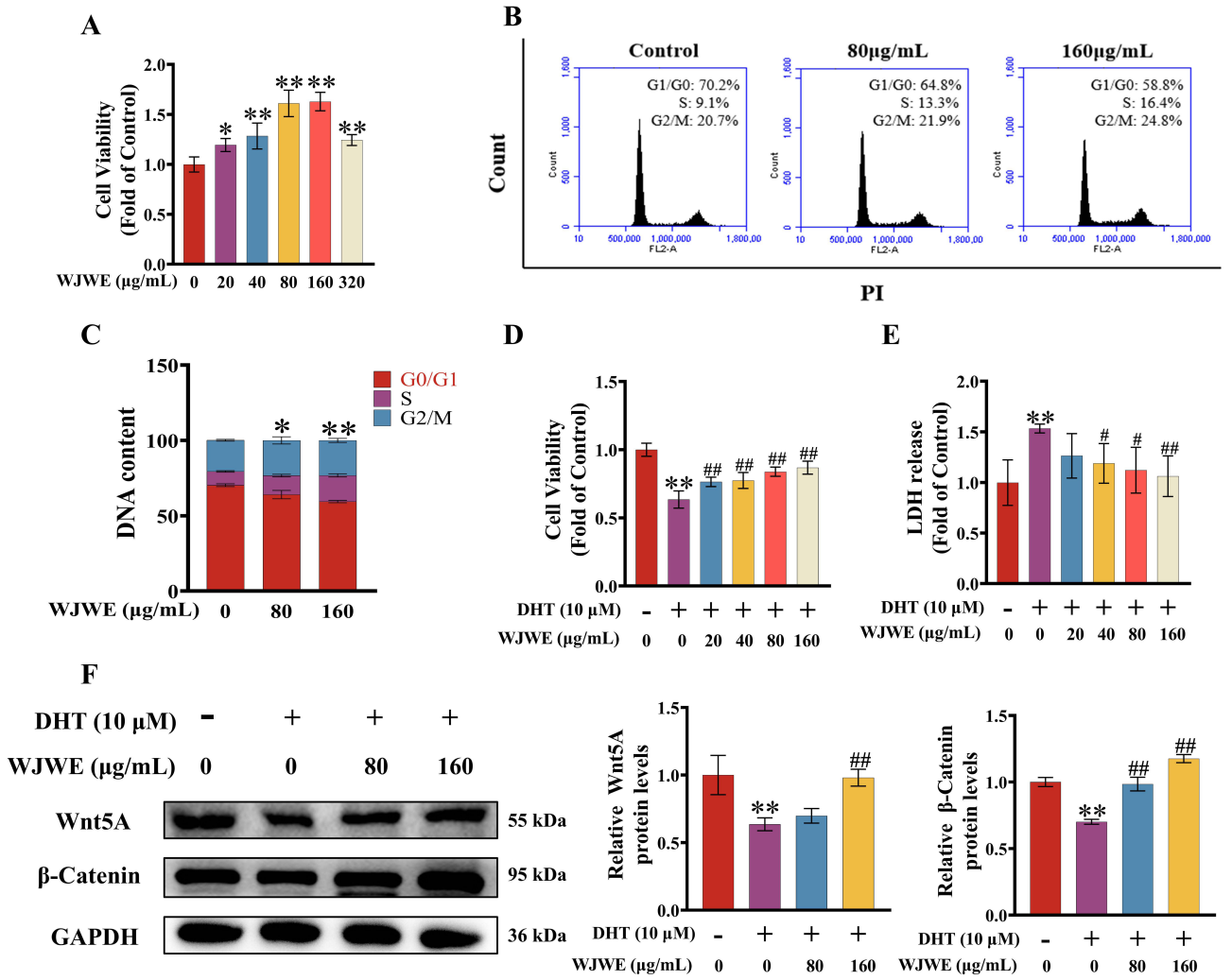

Figure 3 WJWE stimulated the DPCs proliferation and attenuated DHT-induced cell damage in vitro. (**A**) The relative cell viability gradually increased; (**B** and **C**) the analysis of the cell cycling phases of 80, 160 μg/mL WJWE treated DPCs, compared with solvent treated assay (n = 6). (**D**) The increased relative cell viabilities and (**E**) decreased LDH release in different cell assays (n = 6); (**F**) the expression of β-Catenin and Wnt5A (n = 3). Results are presented as means ± SEM. *p < 0.05, **p < 0.01 vs untreated DPCs assay group. #p < 0.05, ##p < 0.01 vs DHT group.

stimulated oxidative stress in DPCs were subsequently determined. Compared with untreated DPCs, the obviously increased ROS (Figure 4B) and MDA (Figure 4C) levels could be observed in DHT-treated DPCs. On the contrary, GSH (Figure 4D) and SOD (Figure 4E) levels were significantly decreased. And WJWE dose dependently attenuated the effects of DHT.

To confirm our findings, we comparatively examined the levels of MDA, GSH and SOD (Figure 4F–H), as well as the expression of cyclooxygenase 2 (COX-2) and heme oxygenase 1 (HO-1) (Figure 4I and J), in the dorsal skin of different murine groups. And the result provided similar events. Together, these results indicated that WJWE could effectively reverse oxidative stress in the DHT-induced models in vitro and in vivo. Next, we explored the regulative capability of WJWE on SIRT1.

WJWE Regulated the SIRT1/JNK/p38 MAPK Pathway in vitro and in vivo

Then, we comparatively determined the expression of SIRT1, phosphorylated JNK and p38 MAPK in different group mice. Compared to the model group, we observed a significantly increased SIRT1 in the hair follicles (particularly in the dermal papilla region) of mice from the Fin, WJL, and WJH groups. Simultaneously, the phosphorylation of both JNK and p38 was significantly decreased (Figures 5A and S1C). In vitro, DHT-exposed DPCs exhibited reduced SIRT1 and

https://doi.org/10.2147/DDDT.S501823

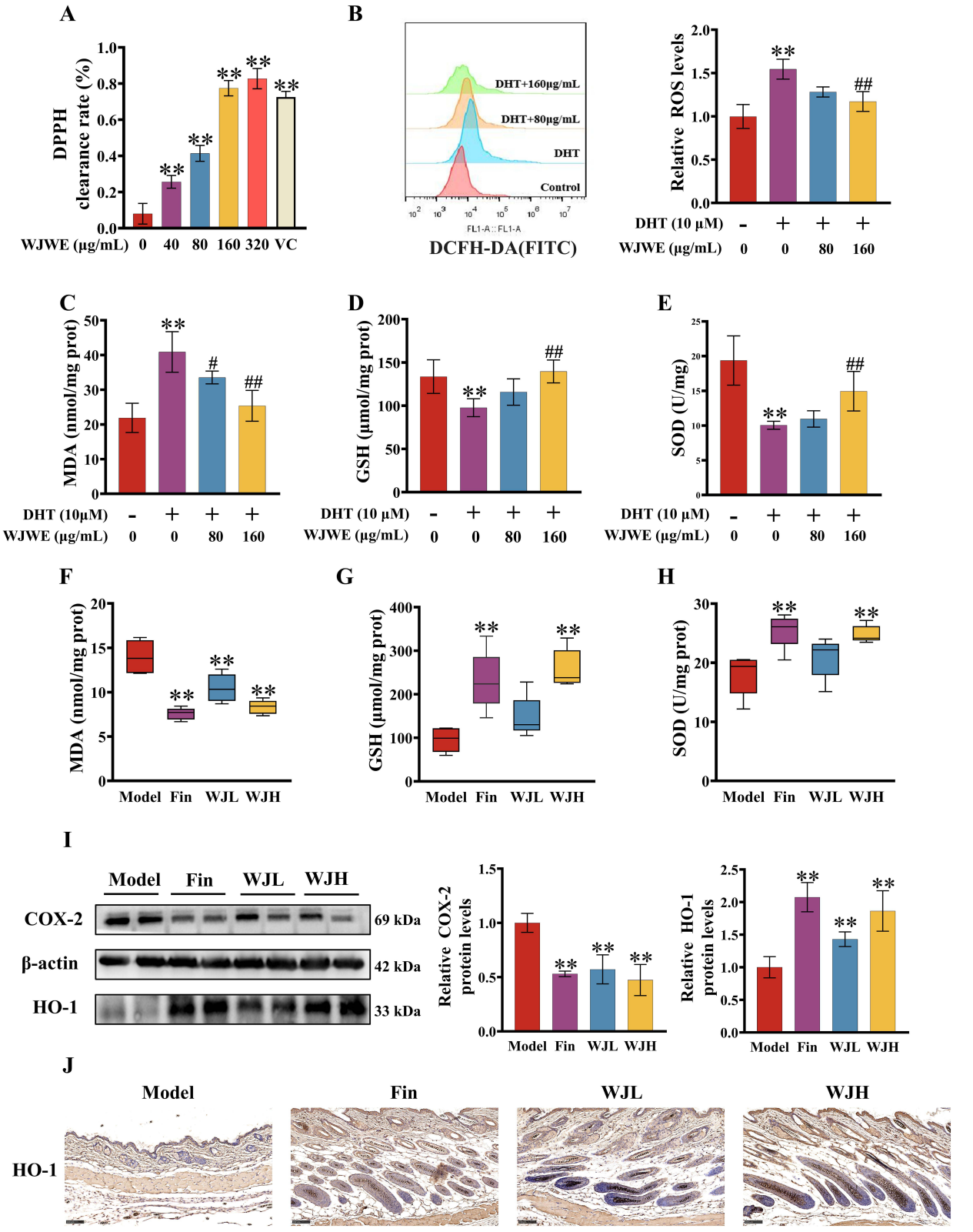

Figure 4 WJWE relieved DHT-induced oxidative stress. (**A**) The free radical clearing activity of WJWE, in comparison with that of vitamin C (n = 6). The antioxidative capability of WJWE were identified with DHT treated DPCs assay: the levels of ROS (**B**), MDA (**C**), GSH (**D**) and SOD (**E**) were significantly reduced by WJWE application (n = 6). And in vivo, the WJWE reduced the DHT-increased high contents of MDA (**F**), GSH (**G**) and SOD (**H**) (n = 5), and ameliorated the DHT induced abnormal expression of COX-2 and HO-1 (**I**) in murine skin (n = 5); (**J**) the immunohistochemical stained HO-1 in the dorsal skin slices shown highly expressed HO-1 in WJL and WJH groups (scale bars = 100 μm, n = 5). Results are presented as means ± SEM. $^{**}p < 0.01$ vs untreated DPCs assay or model group. $^{\#}p < 0.05$, $^{\#\#}p < 0.01$ vs DHT group.

 https://doi.org/10.2147/DDDT.S501823

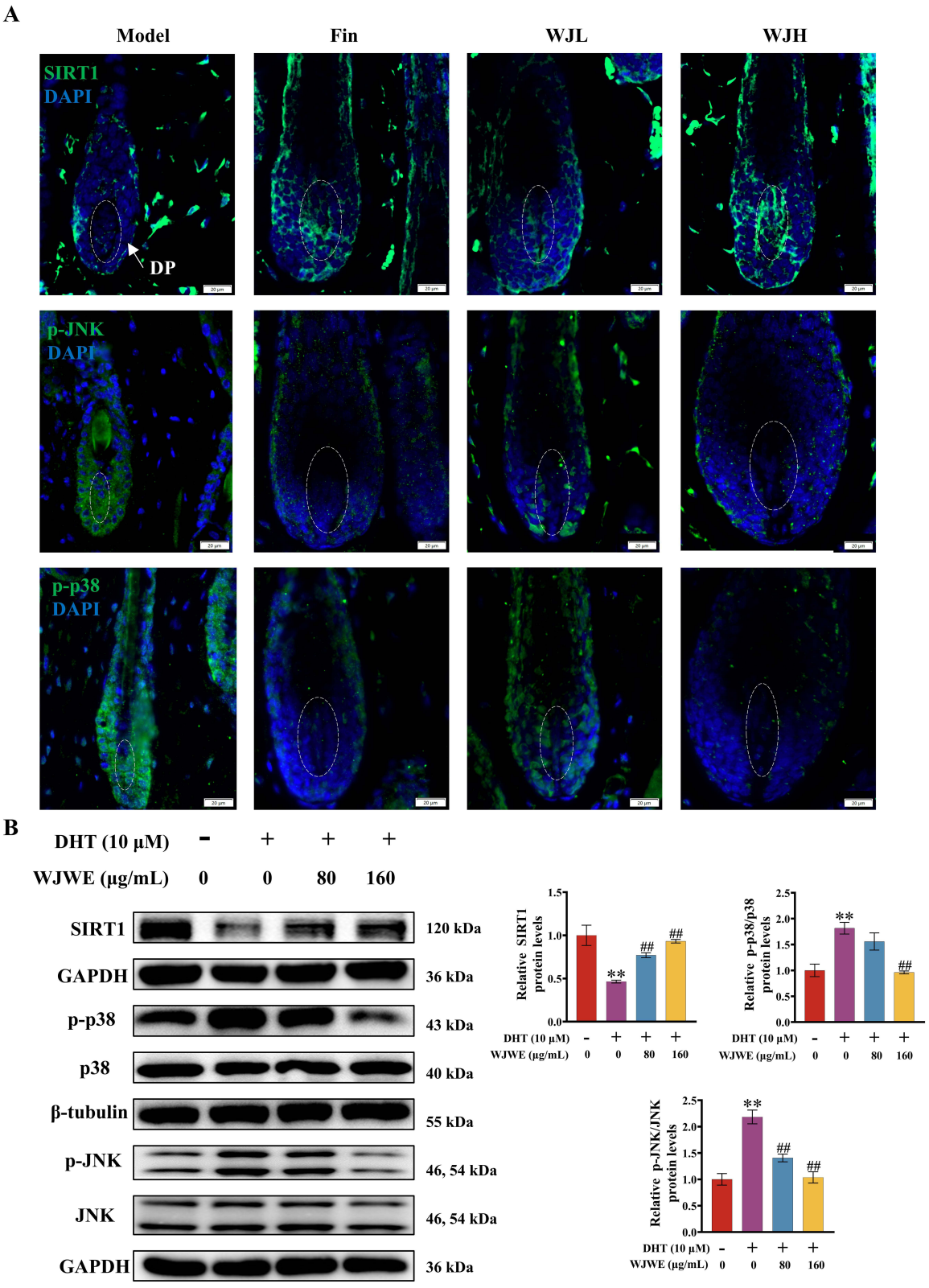

Figure 5 WJWE regulated the DHT-influenced expression of SIRT1/JNK/p38 MAPK. (**A**) The SIRT1, p-JNK, p-p38 in the dorsal skin slices was detected with immunofluorescent staining and observed (scale bars = 20 μm, n = 5); the expression of SIRT1, p-JNK, JNK, p-p38, p38 i in DPCs assays (n = 3) (**B**) were evaluated with specific antibodies, respectively. Results are presented as means ± SEM. **p < 0.01 vs untreated DPCs assay group. ##p < 0.01 vs DHT group.

https://doi.org/10.2147/DDDT.S501823

elevated p-JNK/p-p38 levels, which were dose-dependently reversed by WJWE treatment (Figure 5B). These data strongly support that WJWE mitigates DHT-driven oxidative damage through SIRT1-mediated repression of JNK/p38 MAPK activation.

Treatment with a SIRT1 Inhibitor Abolished the Anti-AGA Effect of WJWE

To validate our finding, we treated the mice with EX527, a SIRT1 inhibitor, to blocking the effects of WJWE. As expected, EX527 treatment attenuated the beneficial effect of the WJWE on the hair growth of AGA model mice (Figure 6A). The dermal thickness and density of hair follicles were also decreased in the EX527 treatment group, compared with the WJH group (Figure 6B–D). Additionally, we verified that the attenuative effect of EX527 on WJWE improved the SOD, GSH and MDA contents (Figure 6E–G), the expression of SIRT1, and the levels of phosphorylated JNK and p38 in the dorsal skin (Figure 6H). These results indicated that the administration of the inhibitor of SIRT1 attenuated the effects of WJWE.

Discussion

AGA is one of the most common types of hair loss, characterized by progressive follicles miniaturization, which is the result of DHT shortened anagen period of hair growth.[24] Although the clinical application of finasteride can improve AGA. The unwished recurrence after the discontinuation of treatment and side effects keep remaining the significant challenges for dermatologists.[25] Some TCM formulas or herbal extracts have been successfully applied in AGA treatment.[14,26] T In Compendium of Materia Medica (Bencao Gangmu), a monograph of TCM, Honghua and Cebaiye have the effect of nourishing kidney essences. Sangshen and Heshouwu can nourish "Qi", "Yin" and tonify blood. And Heizhima, friendly to grey hair, shows multiple health benefit effects, such as nourishing the liver and kidneys, enriching essence and blood (http://www.zysj.com.cn). And evidences indicated that Mohanlian,[27] Honghua[28] and Cebaiye,[29] can improve hair regeneration. Additionally, Sangshen[30] and Heshouwu[24] have been found, which can influence the growth cycle of DPCs and prevent hair loss. Hence, we created a new formula, "Jiawei Erzhiwan" by combining Honghua, Sangshen, Heshouwu, Huangjing, Cebaiye and Heizhima with Mohanlian and Nvzhenzi to increasing the effect of "Erzhiwan" on hair growth. And the excellent improvement efficiency of the WJWE on AGA patient[15] encouraged us to elucidate the underlining mechanism.

We found that WJWE effectively promoted hair growth in AGA model mice (Figure 2), promoted the proliferation of DPCs and protected the DHT-reduced cell viability (Figure 3), by which Wnt/β-Catenin pathway has been stimulated. Subsequent study showed WJWE protected DHT triggered oxidative stress in DPC cells and in AGA mice (Figure 4), by stimulating the expression of SIRT1 and attenuating the phosphorylation of JNK and p38 MAPK (Figure 5). The results suggested that SIRT1/JNK/p38 MAPK pathway might be the key target of WJWE. To verify our finding, the SIRT1 inhibitor EX527 was applied, which inhibited the beneficial effects of WJWE on both hair growth and oxidative stress (Figure 6).

It has been reported that content of DHT is significantly higher in AGA patients than in healthy individuals.[31] DPCs, located in the basal part of the hair follicle, play a vital role in hair growth and regeneration.[32] To our knowledge, the DHT-AR complex in the nucleus drives the variation in autocrine and paracrine factors produced by scalp DPCs and leads to follicle miniaturization and alteration of the hair follicle cycle, by which the expression of Wnt and β-Catenin has been attenuated.[33–35] Hence, in our study, we engaged the DPCs for in vitro studies. A previous study showed that DHT triggered an increase in the level of reactive oxygen species (ROS).[36] And oxidative stress is also a vital event influencing the proliferation of DPCs in AGA patients.[23] In fact, oxidative stress negatively regulates the expression of β-Catenin could attenuate the Wnt pathway.[37] Therefore, we evaluated the ROS, MDA, GSH and SOD levels in DHT treated DPCs, as well as in AGA murine skin (Figure 4). Additionally, in cell- and mice basis, WJWE showed significantly amelioration effects. We also assessed the improving efficiency of WJWE on the expression of HO-1 and COX-2 in AGA mice (Figure 4I and J). HO-1 is an important antioxidative protein, which has been proved to improving hair and skin health.[38] On the contrary, high level of COX-2 indicates the oxidative stress induced inflammatory responses in skin, and also the defected follicle stem cells differentiation.[39]

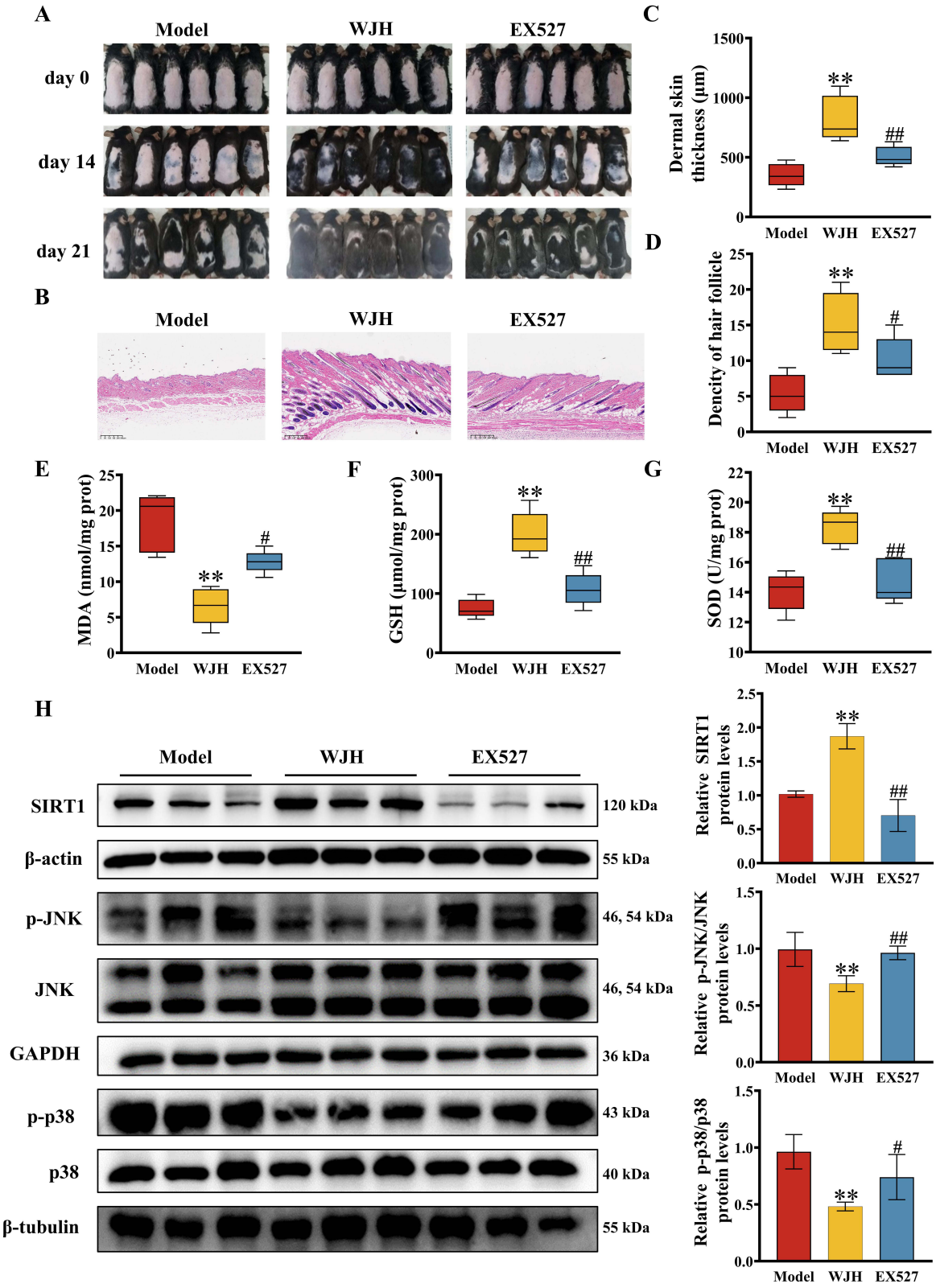

Figure 6 Application of EX527 attenuated the improving activities of WJWE on DHT-induced AGA model mice. (**A**) The photographs of dorsal skins on days 0, 14, and 21 represented that EX527 inhibited the WJH stimulated hair growth in AGA model mice (n = 6); (**B**) the skin slices of different group mice were H&E-stained and observed (scale bars = 300 μm, (n = 5), in which the skin thickness (**C**) and the density of hair follicle (**D**) were quantified (n = 5); the application of EX527 reversed the WJH regulated the levels of SOD (**E**), GSH (**F**) and MDA (**G**) in AGA murine skin (n = 5), and blocked the regulative activity of WJWE on the SIRT1, p-JNK, and p-p38 (n = 6) (**H**). Results are presented as means ± SEM. $^{**}p < 0.01$ vs model group. $^{\#}p < 0.05$, $^{\#\#}p < 0.01$ vs WJH group.

https://doi.org/10.2147/DDDT.S501823

Although various signaling pathways involve in the regulating of hair follicle generation and hair growth, such as Keap1-Nrf2 pathway,[40] Akt-β-Catenin pathway,[40] NF-κB[29] and MAPK,[16,41,42] et al. DHT has been shown to induce mitochondrial oxidative stress by activating p38 MAPK,[43] and also a modulator of JNK.[44] SIRT1 is a key regulator influencing the phosphorylation of JNK and p38 MAPK.[45–47] A recent study showed evidences that SIRT1 involved in alopecia areata.[17] But few evidence of SIRT1/MAPK/JNK pathway in the development of AGA. Hence, in this study, we provide essential evidence of the regulatory effect of WJWE on the SIRT1/JNK/p38 MAPK pathway via in vivo and in vitro experiments (Figures 5A, B and S1B). To demonstrate, SIRT1 is a vital target of WJWE. We administered the SIRT1 inhibitor, EX527, to WJWE-treated AGA model mice, and found that EX527 attenuated the ability of WJWE to regulate hair growth (Figure 6). Consistent with these findings, EX527 prevented the protective and regulatory effects of WJWE on AGA model mice, which provide solid evidence to prove SIRT1 involved in the pathological processes of DHT induced AGA.

While our study focuses on male AGA, the findings may also apply to female androgenetic alopecia (FAGA). FAGA, characterized by diffuse hair thinning in the vertex region, shares similar mechanisms with male AGA, including elevated hormonal levels and altered androgen receptor activity.[1,48] According to WJWE's efficacy in mitigating DHT-induced follicular miniaturization and oxidative stress in our AGA model, we proposed that it may also benefit to FAGA patients by targeting these pathways. However, a FAGA murine model should be engaged. Currently, our group are focusing on investigating hair loss in postmenopausal women, which shares certain overlapping mechanisms with FAGA. Postmenopausal hair loss is dependent on hormonal changes, particularly a decline in estrogen levels, which may lead to an increased influence of androgens on hair follicles. WJWE, containing numerous compounds with estrogen-like activity, has shown efficacy in alleviating postmenopausal hair loss in our preliminary study (unpublished). Our ongoing research aims to further evaluating the AGA and FAGA improving capability of WJWE and to elucidating the underlining mechanisms, which would improve the application of WJWE.

To conclude, this study provided some experimental evidence, in DHT induced murine model and the DPCs assays, to elucidate the mechanism, by which WJWE ameliorated AGA. We found that WJWE improved AGA by promoting hair follicle growth and eliminating DHT-induced oxidative stress in DHT induced murine model. And the result of immunofluorescence staining indicated that SIRT1 should be the key target of the WJWE-regulated signaling network, which negatively regulated the phosphorylation of JNK and p38 MAPK, especially in DPCs (Figure 7).

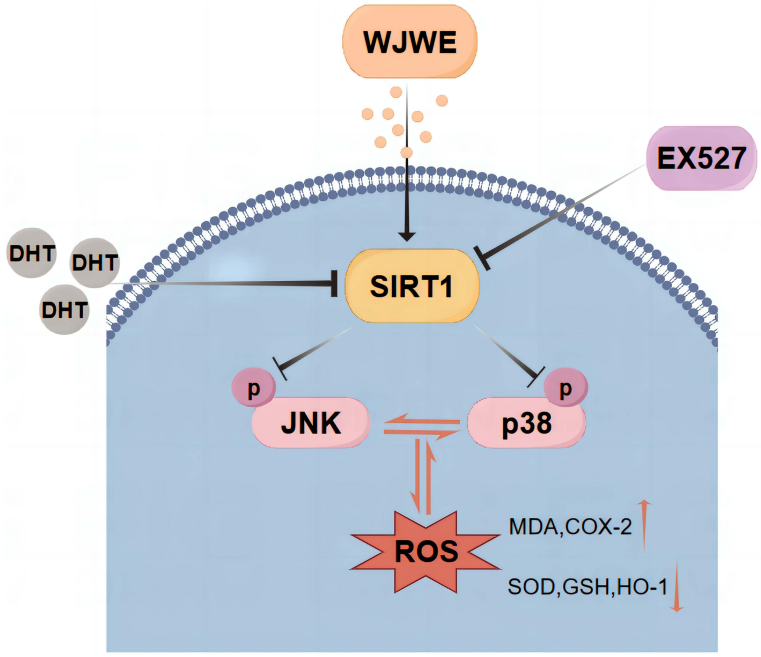

Figure 7 The schematic diagram of the regulative mechanism of WJWE on DHT-induced AGA.

Abbreviations

AA, alopecia areata; AGA, androgenetic alopecia; ANOVA, one-way analysis of variance; AR, androgen receptor; BPI, base peak intensity; CCK-8, cell counting Kit-8; COX-2, cyclooxygenase-2; DHT, dihydrotestosterone; DPCs, dermal papilla cells; DPPH, 2,2-Diphenyl-1-picrylhydrazyl; ECL, enhanced chemiluminescence; EX527, SIRT1 inhibiter treated group; FDA, Food and Drug Administration; GSH, glutathione; H&E, hematoxylin and eosin; HFSCs, hair follicle stem cells; HO-1, heme oxygenase 1; IGF1, insulin-like growth factor 1 receptor; JNK, c-Jun N-terminal kinase; K15, Keratin 15; LDH, lactate dehydrogenase; LEF1, lymphoid Enhancer-Binding Factor; MAPK, mitogen activated protein kinase; MDA, malondialdehyde; MRM, multiple reaction monitoring; ORS, outer root sheath; p38 MAPK, p38 mitogen-activated protein kinase; PPI, protein-protein interaction; PVDF, polyvinylidene fluoride; qRT-PCR, quantitative real-time polymerase chain reaction; ROS, reactive oxygen species; SIRT1, silent information regulator 1; SOD, superoxide dismutase; TIC, total ion current chromatograms; TCM, traditional Chinese medicine); VEGF, vascular endothelial growth factor.

Data Sharing Statement

All data or resources used in the paper are available by reasonable requirements to the correspondence authors. The original data presented in the study are openly available in [FigShare] at [doi: 10.6084/m9.figshare.27059740].

Ethics Approval and Informed Consent

This study was reviewed and approved by the Animal Ethical and Welfare Committee of Zhejiang Chinese Medical University with the approval number: IACUC-20221128-05, dated 2022.11.28. All animal experiments were performed following ethical standards and ARRIVE guidelines.

Acknowledgments

We appreciate the great help from Medical Research Center, Academy of Chinese Medical Sciences, Zhejiang Chinese Medical University. We still thank three of our best friends, Prof. Li Xu, Ms. Jinjun Ji and Prof. Songtao Li, for their great help and valuable suggestions. We also thank for the kindly financial support of Hangzhou Zhimo biotechnology Co., Ltd.

Author Contributions

All authors made a significant contribution to the work reported, whether that is in the conception, study design, execution, acquisition of data, analysis and interpretation, or in all these areas; took part in drafting, revising or critically reviewing the article; gave final approval of the version to be published; have agreed on the journal to which the article has been submitted; and agree to be accountable for all aspects of the work.

Funding

This work was supported by National Natural Science Foundation of China [No. 82305239]; Zhejiang Province Traditional Chinese Medicine Science and Technology Plan Project [No. 2023ZF011 and No. 2020ZB082]; the Scientific Research Improving Project of Life Sciences College of Zhejiang Chinese Medical University [No. 2022ZY001]; the Basic Public Welfare Research Projects of Zhejiang Province [No. LY21H270005]; the Zhejiang Science and Technology Innova-tion Program [No. 023R41059].

Disclosure

The authors declare that the research was conducted in the absence of any commercial or financial relationships that could be construed as a potential conflict of interest.

References

1. Sawaya ME, Price VH. Different levels of 5alpha-reductase type I and II, aromatase, and androgen receptor in hair follicles of women and men with androgenetic alopecia. *J Invest Dermatol*. 1997;109(3):296–300.
2. Gilliver SC, Ruckshanthi JPD, Hardman MJ, Zeef LAH, Ashcroft GS. 5alpha-dihydrotestosterone (DHT) retards wound closure by inhibiting re-epithelialization. *J Pathol*. 2009;217(1):73–82. doi:10.1002/path.2444
3. Steindl-Kuscher K, Krugluger W, Boulton ME, et al. Activation of the beta-catenin signaling pathway and its impact on RPE cell cycle. *Invest Ophthalmol Vis Sci*. 2009;50(9):4471–4476. doi:10.1167/iovs.08-3139
4. Falih IQ. The effect of ferritin, vitamin D, and some hormonal and biochemical parameters on patients with female-pattern hair loss after COVID-19 infection. *J Prev Diagn Treat Strategies Med*. 2023;2(4):218–223. doi:10.4103/jpdtsm.jpdtsm_108_23
5. Tabolli S, Sampogna F, Di Pietro C, Mannooranparampil TJ, Ribuffo M, Abeni D. Health status, coping strategies, and alexithymia in subjects with androgenetic alopecia: a questionnaire study. *Am J Clin Dermatol*. 2013;14(2):139–145. doi:10.1007/s40257-013-0010-3
6. Adil A, Godwin M. The effectiveness of treatments for androgenetic alopecia: a systematic review and meta-analysis. *J Am Acad Dermatol*. 2017;77(1). doi:10.1016/j.jaad.2017.02.054
7. Tu Y. Artemisinin-A gift from traditional Chinese medicine to the world (Nobel Lecture). *Angew Chem Int Ed Engl*. 2016;55(35):10210–10226. doi:10.1002/anie.201601967
8. Min L, Han J-C, Zhang W, Gu -C-C, Zou Y-P, Li -C-C. Strategies and lessons learned from total synthesis of taxol. *Chem Rev*. 2023;123(8):4934–4971. doi:10.1021/acs.chemrev.2c00763
9. Ji C, Ma J, Feng C, et al. Promotion of hair regrowth in androgenetic alopecia with supplemented Erzhi Wan: exploring its mechanism using network pharmacology and molecular docking. *Clin Cosmet Invest Dermatol*. 2023;16:2995–3022. doi:10.2147/CCID.S425295
10. Shang G, Niu X, Tong Q, et al. Integrated metabolomic and lipidomic analysis revealed the protective mechanisms of Erzhi Wan on senescent NRK cells through BRL cells. *J Ethnopharmacol*. 2024;320:117482. doi:10.1016/j.jep.2023.117482
11. Zuo J-Y, Park C, Doschak M, Löbenberg R. Are the release characteristics of Erzhi pills in line with traditional Chinese medicine theory? A quantitative study. *J Integr Med*. 2021;19(1):50–55. doi:10.1016/j.joim.2020.10.004
12. Cheng M, Wang Q, Fan Y, et al. A traditional Chinese herbal preparation, Er-Zhi-Wan, prevent ovariectomy-induced osteoporosis in rats. *J Ethnopharmacol*. 2011;138(2):279–285. doi:10.1016/j.jep.2011.09.030
13. Zhai Y, Xu J, Feng L, et al. Broad range metabolomics coupled with network analysis for explaining possible mechanisms of Er-Zhi-Wan in treating liver-kidney Yin deficiency syndrome of Traditional Chinese medicine. *J Ethnopharmacol*. 2019;234:57–66. doi:10.1016/j.jep.2019.01.019
14. Zhang B, Zhang R-W, Yin X-Q, et al. Inhibitory activities of some traditional Chinese herbs against testosterone 5α-reductase and effects of Cacumen platycladi on hair re-growth in testosterone-treated mice. *J Ethnopharmacol*. 2016;177:1–9. doi:10.1016/j.jep.2015.11.012
15. Qian Y, Zhu L, Wu L, et al. Favorable effect of herbal extract on androgenic alopecia: a case report. *Medicine*. 2023;102(39):e34524. doi:10.1097/MD.0000000000034524
16. Liu J, Xu Y, Wu Q, Ding Q, Fan W. Sirtuin-1 protects hair follicle stem cells from TNFα-mediated inflammatory stress via activating the MAPK-ERK-Mfn2 pathway. *Life Sci*. 2018;212:213–224. doi:10.1016/j.lfs.2018.10.003
17. Hao L, Nam K-H, Lee G-J, et al. SIRT1 downregulation provokes immune-inflammatory responses in hair follicle outer root sheath cells and may contribute to development of alopecia areata. *J Dermatol Sci*. 2023;111(1):2–9. doi:10.1016/j.jdermsci.2023.05.005
18. Huang X, Shi Y, Chen H, et al. Isoliquiritigenin prevents hyperglycemia-induced renal injuries by inhibiting inflammation and oxidative stress via SIRT1-dependent mechanism. *Cell Death Dis*. 2020;11(12):1040. doi:10.1038/s41419-020-03260-9
19. Yuan A, Xia F, Bian Q, et al. Ceria nanozyme-integrated microneedles reshape the perifollicular microenvironment for androgenetic alopecia treatment. *ACS Nano*. 2021;15(8):13759–13769. doi:10.1021/acsnano.1c05272
20. Jung YH, Chae CW, Choi GE, et al. Cyanidin 3-O-arabinoside suppresses DHT-induced dermal papilla cell senescence by modulating p38-dependent ER-mitochondria contacts. *J Biomed Sci*. 2022;29(1):17. doi:10.1186/s12929-022-00800-7
21. Chen X, Liu B, Li Y, et al. Dihydrotestosterone regulates hair growth through the Wnt/β-Catenin pathway in C57BL/6 mice and in vitro organ culture. *Front Pharmacol*. 2019;10:1528. doi:10.3389/fphar.2019.01528
22. Zhang Y, Huang J, Fu D, et al. Transcriptome analysis reveals an inhibitory effect of dihydrotestosterone-treated 2D- and 3D-cultured dermal papilla cells on hair follicle growth. *Front Cell Dev Biol*. 2021;9:724310. doi:10.3389/fcell.2021.724310
23. Upton JH, Hannen RF, Bahta AW, Farjo N, Farjo B, Philpott MP. Oxidative stress-associated senescence in dermal papilla cells of men with androgenetic alopecia. *J Invest Dermatol*. 2015;135(5):1244–1252. doi:10.1038/jid.2015.28
24. Shin JY, Choi Y-H, Kim J, et al. Polygonum multiflorum extract support hair growth by elongating anagen phase and abrogating the effect of androgen in cultured human dermal papilla cells. *BMC Complement Med Ther*. 2020;20(1):144. doi:10.1186/s12906-020-02940-5
25. Varothai S, Bergfeld WF. Androgenetic alopecia: an evidence-based treatment update. *Am J Clin Dermatol*. 2014;15(3):217–230. doi:10.1007/s40257-014-0077-5
26. Fang T, Xu R, Sun S, et al. Caizhixuan hair tonic regulates both apoptosis and the PI3K/Akt pathway to treat androgenetic alopecia. *PLoS One*. 2023;18(2):e0282427. doi:10.1371/journal.pone.0282427
27. Lee K-H, Choi D, Jeong S-I, et al. Eclipta prostrata promotes the induction of anagen, sustains the anagen phase through regulation of FGF-7 and FGF-5. *Pharm Biol*. 2019;57(1):105–111. doi:10.1080/13880209.2018.1561729
28. Junlatat J, Sripanidkulchai B. Hair growth-promoting effect of Carthamus tinctorius floret extract. *Phytother Res*. 2014;28(7):1030–1036. doi:10.1002/ptr.5100
29. Fu H, Li W, Weng Z, et al. Water extract of cacumen platycladi promotes hair growth through the Akt/GSK3β/β-catenin signaling pathway. *Front Pharmacol*. 2023;14:1038039. doi:10.3389/fphar.2023.1038039
30. Hyun J, Im J, Kim S-W, Kim HY, Seo I, Bhang SH. Morus alba root extract induces the anagen phase in the human hair follicle dermal papilla cells. *Pharmaceutics*. 2021;13(8). doi:10.3390/pharmaceutics13081155
31. Hobo Y, Nishikawa J, Taniguchi Asai N, et al. Evaluation of the therapeutic effects of AGA drugs by measuring finasteride, dutasteride, and dihydrotestosterone in hair. *Clin Chim Acta*. 2023;547:117456. doi:10.1016/j.cca.2023.117456
32. Kim SM, Kang J-I, Yoon H-S, et al. HNG, A humanin analogue, promotes hair growth by inhibiting anagen-to-catagen transition. *Int J Mol Sci*. 2020;21(12). doi:10.3390/ijms21124553

33. Moon IJ, Yoon HK, Kim D, et al. Efficacy of asymmetric siRNA targeting androgen receptors for the treatment of androgenetic alopecia. *Mol Pharm*. 2023;20(1):128–135. doi:10.1021/acs.molpharmaceut.2c00510
34. Kwack MH, Sung YK, Chung EJ, et al. Dihydrotestosterone-inducible dickkopf 1 from balding dermal papilla cells causes apoptosis in follicular keratinocytes. *J Invest Dermatol*. 2008;128(2):262–269.
35. Fu H, Li W, Liu J, et al. Ellagic acid inhibits dihydrotestosterone-induced ferroptosis and promotes hair regeneration by activating the wnt/β-catenin signaling pathway. *J Ethnopharmacol*. 2024;330:118227. doi:10.1016/j.jep.2024.118227
36. Jin B-R, Lim C-Y, Kim H-J, Lee M, An H-J. Antioxidant mitoquinone suppresses benign prostatic hyperplasia by regulating the AR-NLRP3 pathway. *Redox Biol*. 2023;65:102816. doi:10.1016/j.redox.2023.102816
37. Shin SY, Kim CG, Jho E-H, et al. Hydrogen peroxide negatively modulates Wnt signaling through downregulation of beta-catenin. *Cancer Lett*. 2004;212(2):225–231.
38. Zhao P, Park NH, Alam MB, Lee S-H. Fuzhuan brick tea boosts melanogenesis and prevents hair graying through reduction of oxidative stress via NRF2-HO-1 signaling. *Antioxidants*. 2022;11(3). doi:10.3390/antiox11030599
39. Mathur AN, Zirak B, Boothby IC, et al. Treg-cell control of a CXCL5-IL-17 inflammatory axis promotes hair-follicle-stem-cell differentiation during skin-barrier repair. *Immunity*. 2019;50(3). doi:10.1016/j.immuni.2019.02.013
40. Peterle L, Sanfilippo S, Borgia F, Cicero N, Gangemi S. Alopecia areata: a review of the role of oxidative stress, possible biomarkers, and potential novel therapeutic approaches. *Antioxidants*. 2023;12(1). doi:10.3390/antiox12010135
41. Liu X, Zhang P, Zhang X, et al. Fgf21 knockout mice generated using CRISPR/Cas9 reveal genetic alterations that may affect hair growth. *Gene*. 2020;733:144242. doi:10.1016/j.gene.2019.144242
42. Li K, Sun Y, Liu S, et al. The AR/miR-221/IGF-1 pathway mediates the pathogenesis of androgenetic alopecia. *Int J Biol Sci*. 2023;19 (11):3307–3323. doi:10.7150/ijbs.80481
43. Xu Z-R, Hu L, Cheng L-F, Qian Y, Yang Y-M. Dihydrotestosterone protects human vascular endothelial cells from H_2O_2-induced apoptosis through inhibition of caspase-3, caspase-9 and p38 MAPK. *Eur J Pharmacol*. 2010;643(2–3):254–259. doi:10.1016/j.ejphar.2010.06.039
44. Altuwaijri S, Lin H-K, Chuang K-H, et al. Interruption of nuclear factor kappaB signaling by the androgen receptor facilitates 12-O-tetradecanoylphorbolacetate-induced apoptosis in androgen-sensitive prostate cancer LNCaP cells. *Cancer Res*. 2003;63(21):7106–7112.
45. Becatti M, Taddei N, Cecchi C, Nassi N, Nassi PA, Fiorillo C. SIRT1 modulates MAPK pathways in ischemic-reperfused cardiomyocytes. *Cell Mol Life Sci*. 2012;69(13):2245–2260. doi:10.1007/s00018-012-0925-5
46. Li D, Liu N, Zhao -H-H, et al. Interactions between Sirt1 and MAPKs regulate astrocyte activation induced by brain injury in vitro and in vivo. *J Neuroinflammation*. 2017;14(1):67. doi:10.1186/s12974-017-0841-6
47. Alves-Fernandes DK, Jasiulionis MG. The role of SIRT1 on DNA damage response and epigenetic alterations in cancer. *Int J Mol Sci*. 2019;20(13). doi:10.3390/ijms20133153
48. Devjani S, Ezemma O, Kelley KJ, Stratton E, Senna M. Androgenetic alopecia: therapy update. *Drugs*. 2023;83(8):701–715. doi:10.1007/s40265-023-01880-x